




1994

Interaction of Platinum Films with the (0001[#]) and (0001) Surfaces of ZnO

W. T. Petrie
University of Pennsylvania

John M. Vohs
University of Pennsylvania, vohs@seas.upenn.edu

Follow this and additional works at: http://repository.upenn.edu/cbe_papers

 Part of the [Biochemical and Biomolecular Engineering Commons](#), [Materials Science and Engineering Commons](#), and the [Polymer Science Commons](#)

Recommended Citation

Petrie, W. T., & Vohs, J. M. (1994). Interaction of Platinum Films with the (0001[#]) and (0001) Surfaces of ZnO. *The Journal of Chemical Physics*, 101 8098-8107. <http://dx.doi.org/10.1063/1.468237>

This paper is posted at ScholarlyCommons. http://repository.upenn.edu/cbe_papers/179
For more information, please contact repository@pobox.upenn.edu.

Interaction of Platinum Films with the (0001#) and (0001) Surfaces of ZnO

Abstract

In this investigation, the growth, structure, and electronic properties of Pt films on the polar surfaces of ZnO were examined using high-resolution electron energy-loss spectroscopy (HREELS) and low-energy, electron diffraction (LEED). The growth mode of vapor-deposited Pt films on ZnO(0001#) and ZnO(0001) at 300 K was found to be nearly layer-by-layer. The surfaces of Pt films produced in this manner exhibited hexagonal symmetry and were stable up to 600 K. At higher temperatures, the Pt agglomerated into particles which remained oriented with respect to the ZnO substrate. HREELS results indicate that there are only weak interactions at the Pt/ZnO(0001#) interface, while charge transfer and Schottky barrier formation occurs at the Pt/ZnO(0001) interface.

Disciplines

Biochemical and Biomolecular Engineering | Chemical Engineering | Engineering | Materials Science and Engineering | Polymer Science

Interaction of platinum films with the (000 $\bar{1}$) and (0001) surfaces of ZnO

W. T. Petrie and J. M. Vohs^{a)}

Department of Chemical Engineering, University of Pennsylvania, Philadelphia, Pennsylvania 19104-6393

(Received 21 April 1994; accepted 22 July 1994)

In this investigation, the growth, structure, and electronic properties of Pt films on the polar surfaces of ZnO were examined using high-resolution electron energy-loss spectroscopy (HREELS) and low-energy, electron diffraction (LEED). The growth mode of vapor-deposited Pt films on ZnO(0001) and ZnO(000 $\bar{1}$) at 300 K was found to be nearly layer-by-layer. The surfaces of Pt films produced in this manner exhibited hexagonal symmetry and were stable up to 600 K. At higher temperatures, the Pt agglomerated into particles which remained oriented with respect to the ZnO substrate. HREELS results indicate that there are only weak interactions at the Pt/ZnO(000 $\bar{1}$) interface, while charge transfer and Schottky barrier formation occurs at the Pt/ZnO(0001) interface.

I. INTRODUCTION

The interface between a metal and a metal oxide is of central importance in a variety of technological applications, including heterogeneous catalysis, microelectronic devices, and composite materials. For this reason, in recent years there have been numerous studies focused on determining the structure and physical properties of metal-metal oxide interfaces. Although there are many approaches available to study these systems, characterization of interfaces produced under the carefully controlled conditions of ultrahigh vacuum has several advantages. Among these are the ability to construct interfaces in an environment free from contamination and access to a variety of *in situ* spectroscopic probes capable of providing electronic and structural information without damaging the sample.

The work presented here involves characterizing the interactions between vapor-deposited Pt films and the (0001) and (000 $\bar{1}$) surfaces of ZnO and focuses on determining how the surface structure of the oxide affects these interactions. ZnO has a wurtzite crystal structure. A schematic representation of the (000 $\bar{1}$) surface is shown in Fig. 1(a). This surface consists of a hexagonal array of oxygen anions (O^{2-}). Zinc cations (Zn^{2+}) in the second layer are not exposed on this surface due to the relatively large size of the O^{2-} ions. Reaction studies carried out on this surface show that it is relatively unreactive toward simple organic molecules, such as alcohols and carboxylic acids.¹⁻⁶ The (0001) surface, shown in Fig. 1(b), has a hexagonal arrangement of Zn^{2+} ions in its outermost layer. Due to the small size of the Zn^{2+} ions, a subsurface layer of O^{2-} ions is also partially exposed on this surface. It has been suggested that exposed cation-anion pairs on this surface are the active sites for the adsorption of a variety of organic molecules.¹⁻⁶ Brønsted acids, such as alcohols, carboxylic acids, and alkynes, adsorb dissociatively on these cation-anion site pairs to form hydroxyl groups and conjugate base anions.

Given the dramatic differences in the reactivity of the two polar surfaces of ZnO toward organic species, variances in the interaction of metal atoms with these surfaces might also be expected. Recent studies by Roberts and Gorte sug-

gest that this may indeed be the case.⁷ These researchers studied Pt-ZnO interface formation on ZnO(0001) and ZnO(000 $\bar{1}$) using Auger electron spectroscopy (AES) and transmission electron microscopy (TEM). They found that vapor-deposited Pt overlayers grew as oriented, two-dimensional films on both surfaces at room temperature. These films were stable at temperatures below 650 K, while at higher temperatures the Pt coalesced into particles. Studies of the thermal desorption behavior of CO on the metal films indicated that there were differences in the chemical reactivity of Pt films supported on the two surfaces. These differences were attributed to interactions between Pt and Zn^{2+} ions on the (0001) surface.

In the present study, the interaction of Pt overlayers with the polar surfaces of ZnO has been further examined using high-resolution electron energy-loss spectroscopy (HREELS) and low-energy electron diffraction (LEED). As will be shown below, the results of this study provide further insight into the growth mechanism of Pt films on ZnO and into the nature of the electronic interactions at the Pt/ZnO interface.

II. EXPERIMENT

Experiments were conducted in an ion-pumped ultrahigh-vacuum chamber equipped with a high-resolution electron energy-loss spectrometer (McAllister Technical Services), LEED/Auger retarding field analyzer (Omicron), mass spectrometer (UTI), and sputter ion gun (Physical Electronics). The background pressure in the chamber was typically 2×10^{-10} Torr. A second ultrahigh vacuum (UHV) chamber with a similar configuration and equipped with a cylindrical mirror analyzer (Omicron), mass spectrometer (UTI), and a sputter ion gun was used to perform AES and reaction studies.

The ZnO single crystal used in this study was approximately 5 mm \times 5 mm \times 2 mm in size and was oriented using Laue x-ray diffraction. The (0001) and (000 $\bar{1}$) polar faces were identified by etching with nitric acid, using the procedure described by Mariano and Hanneman.⁸ The surfaces were mechanically polished until optically smooth using 0.25 μ m diamond paste. The surface was cleaned in vacuum by sputtering with a 500 V Ar^+ ion beam followed by annealing at 950 K. This procedure was repeated until no im-

^{a)} Author to whom correspondence should be addressed.

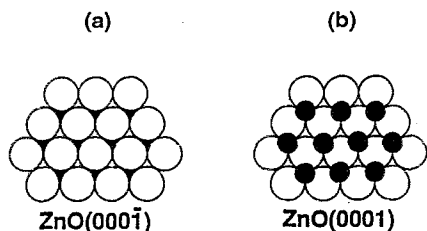


FIG. 1. Schematic representations of the polar surfaces of ZnO. (a) ZnO(000 $\bar{1}$) and (b) ZnO(0001). The open circles represent oxygen anions and the filled circles represent zinc cations.

purities were detected using AES or HREELS and the surface exhibited a sharp 1×1 hexagonal LEED pattern. Removal of deposited Pt multilayers required approximately 2 h of sputtering. The ZnO single crystal was attached to the sample manipulator using a thin piece of tantalum foil wrapped around the back face. Heating and cooling of the crystal were accomplished via conduction through the foil. The temperature of the sample was monitored using a Chromel–Alumel thermocouple attached to the crystal using a vacuum-compatible ceramic adhesive (Aremco #503).

A resistively-heated evaporative metal source was used for Pt deposition and was constructed by wrapping 0.1 mm diam high-purity Pt wire (Johnson Matthey, 99.998%) around a 0.25 mm diam tungsten wire. The tungsten wire was then attached to an electrical feedthrough on the UHV chamber allowing it to be heated resistively. The steady-state flux of Pt was monitored using a quartz crystal oscillator (Maxtek, Inc.) The metal source was operated such that the flux of Pt atoms at the surface of the sample was 1.1×10^{12} atoms/s cm^2 . The temperature of the ZnO substrate was held at 300 K during Pt deposition. Platinum coverages were measured in monolayers. The density of Pt atoms in a monolayer was assumed to be the same as that on a Pt(111) surface, i.e., 1.5×10^{15} atoms/ cm^2 .

HREEL spectra were collected in the specular direction using a 3.5 eV incident electron beam directed 60° from the surface normal. The elastic peak intensity from clean ZnO surfaces was typically 150 kHz. Deposition of a monolayer of Pt reduced this intensity by one to two orders of magnitude. In order to improve the signal to noise ratio, signal averaging of 50 scans was employed. Although the intrinsic resolution of the HREEL spectrometer, as determined by measuring the full-width at half-maximum (FWHM) of the elastic peak in a straight-through geometry, was approximately 5 meV, the best resolution obtained from the clean ZnO surfaces was 10 meV. This relatively low resolution is due to the electrical properties of the ZnO sample. ZnO is an intrinsic n -type semiconductor. The plasma oscillations of the conduction electrons couple with the phonon modes of the substrate, causing both a decrease in intensity and significant broadening of the phonon losses.^{9–12} Because the plasmon dispersion relation extends to zero energy, the elastic peak is broadened as well. Additional decreases in the spectral resolution may have been caused by the presence of steps or defects on the ZnO surface, but their effect was

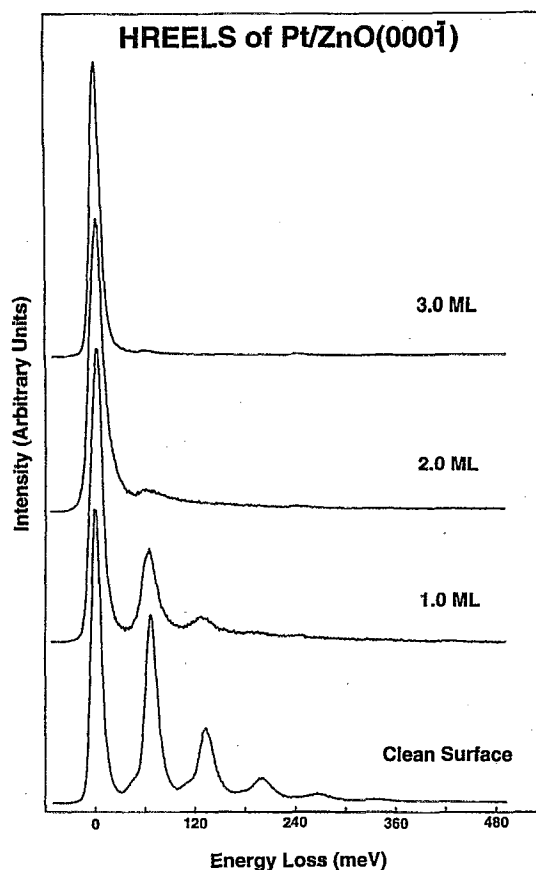


FIG. 2. HREEL spectra of Pt/ZnO(000 $\bar{1}$) as a function of the Pt layer thickness. The bottom spectrum is of the clean surface. The Pt coverage is indicated above each curve. The intensity of each spectrum has been normalized to that of its elastic peak.

presumably much smaller than that of the plasma-phonon coupling.

III. RESULTS

A. Growth of Pt overlayers on ZnO(000 $\bar{1}$)

The HREEL spectrum of the clean ZnO(000 $\bar{1}$) surface is displayed in the lower portion of Fig. 2. This spectrum is in good agreement with those reported previously for ZnO.^{11–15} The large peak at 67.0 meV is due to excitation of a long wavelength surface optical phonon (Fuchs–Kliwer mode). The series of smaller losses which appear at integral multiples of the phonon loss are phonon–phonon combination peaks resulting from sequential excitation of the phonon by a single incident electron. In addition to the phonon losses there is also a small feature centered at 49.6 meV, which appears as a shoulder on the phonon fundamental. The origin of this small feature is not completely clear, however, this mode was not detected in the HREEL spectrum of the (0001) surface. Thus, it is not related to the bulk structure of the oxide. A possible origin of this feature is a vibrational mode localized at defects, such as surface oxygen vacancies.

The remaining HREEL spectra presented in Fig. 2 were collected following deposition of 1, 2, and 3 ML of Pt on the (000 $\bar{1}$) surface. The intensity of the elastic peak in the spec-

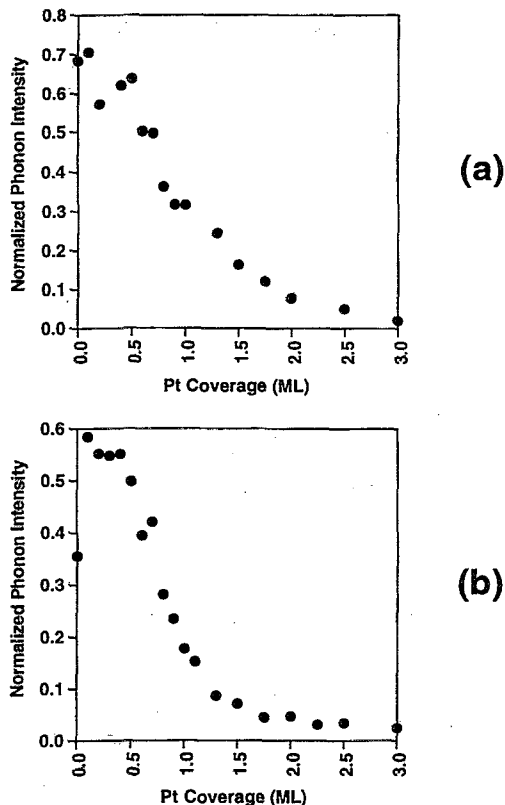


FIG. 3. Ratio of the intensity of the phonon peak to that of the elastic peak as a function of the Pt layer thickness for (a) Pt/ZnO(0001) and (b) Pt/ZnO(0001).

tra of the metal-covered surfaces was approximately 10% of that obtained from the clean surface. Examination of these spectra reveals that significant changes in the relative intensity of the phonon mode and the spectral resolution accompanied Pt deposition. These observations are summarized in Figs. 3(a) and 4(a), where the ratio of the intensity of the phonon peak to that of the elastic peak and the FWHM of the elastic peak are plotted vs Pt coverage for all experimentally measured overlayer thicknesses. One interesting aspect of the HREEL spectra in Fig. 2 is that the small loss feature at 49.6 meV, which was tentatively assigned to surface defects, was not observed for the Pt-covered surfaces, even for coverages as low as 0.1 ML. Assuming that this loss is related to the presence of defects, this result suggests that the first few Pt atoms deposited on the surface are preferentially adsorbed at defect sites. For Pt layers thicker than 3 ML, no further changes in the HREEL spectra were observed.

Figure 3(a) shows that the ratio of the intensity of the phonon fundamental to that of the elastic peak decreased monotonically from a value of 0.68 for the clean surface to 0.02 after deposition of 3 ML of Pt. This demonstrates that the Pt overlayer is quite effective in screening the oscillating dipole of the ZnO surface phonon; this is consistent with the Pt overlayer covering the entire surface, suggesting that the growth is approximately layer-by-layer. Roberts and Gorte arrived at a similar conclusion for this system based on AES and TEM data.⁷

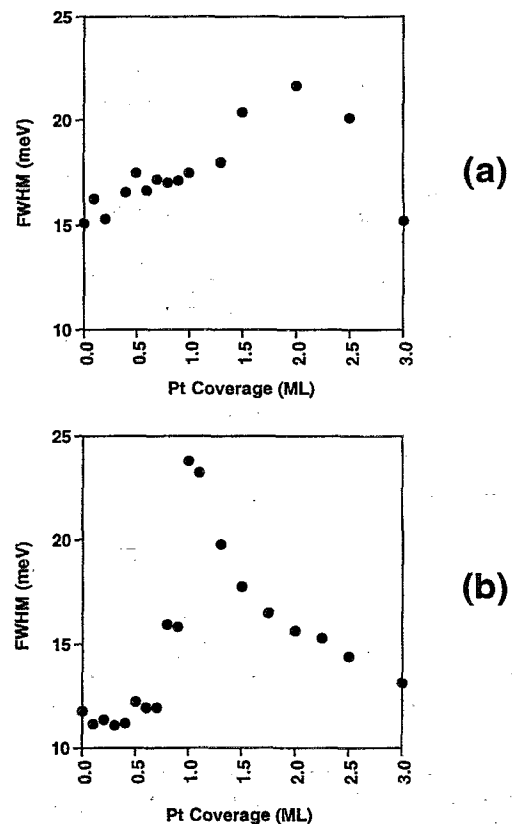


FIG. 4. The full-width at half-maximum (FWHM) of the elastic peak as a function of the Pt layer thickness for (a) Pt/ZnO(0001) and (b) Pt/ZnO(0001).

The FWHM of the elastic peak in the HREEL spectrum of clean ZnO(0001) was 15.1 meV. As shown in Fig. 4(a), this peak width increased roughly linearly with increasing Pt coverage to a maximum value of 21.7 meV for a 2 ML film. Upon deposition of an additional monolayer of Pt, the FWHM decreased to 15.0 meV. Although it has been previously demonstrated that, for the conditions used in this study, the Pt overlayer grows in a layer-by-layer fashion,⁷ it is probably incorrect to assume that the film is completely smooth at the atomic level due to the presence of Pt islands at coverages other than integral multiples of a monolayer. Thus, an increase in the surface roughness resulting from the deposited Pt layer may be responsible for a portion of the decrease in spectral resolution. It is unlikely, however, that the asperity of the overlayer could cause the FWHM of the elastic peak to broaden by 6.2 meV. Indeed as will be shown below, the presence of relatively large Pt particles on the surface results in only a 1.1 meV increase in the FWHM (see Sec. III C). It is more likely that the spectral broadening that accompanies Pt deposition results from scattering from conduction electrons in the thin Pt overlayer. These conduction electrons would be expected to give rise to a plasmonlike mode. For a small density of charge carriers, as would be the case in a monolayer Pt film, the plasmonlike mode would appear as a loss continuum starting at zero meV and extending to higher energies.¹⁶ This loss continuum gives rise to the tail observed on the high energy side of the elastic peak. A

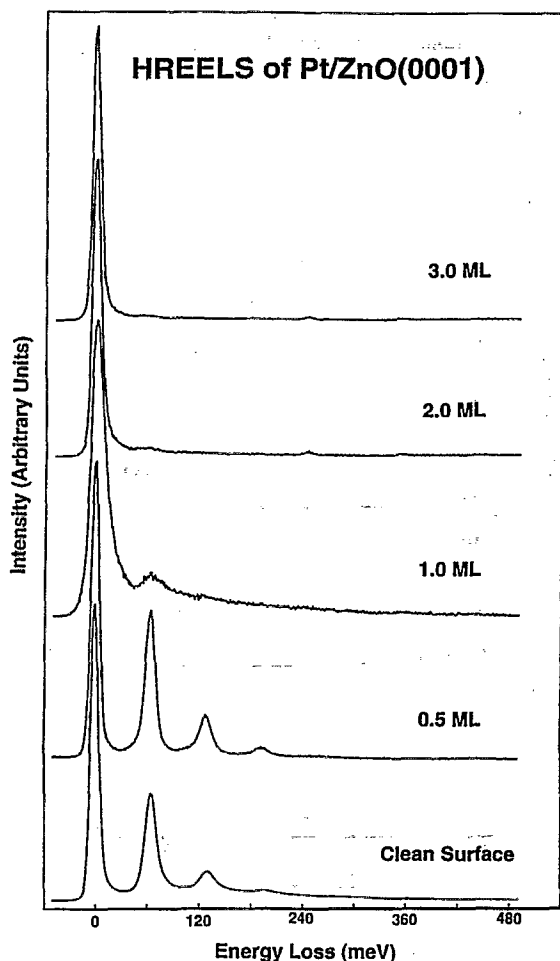


FIG. 5. HREEL spectra of Pt/ZnO(0001) as a function of the Pt layer thickness. The bottom spectrum is of the clean surface. The Pt coverage is indicated above each curve. The intensity of each spectrum has been normalized to that of its elastic peak.

similar effect has been observed in a HREELS study of the interaction of Ag with GaAs(100).¹⁶

As the thickness of the Pt film is increased, its electrical properties eventually approach that of bulk Pt. This results in the disappearance of the low-energy loss continuum associated with the thin Pt layer and the appearance of a discrete plasmon loss. For bulk Pt, the plasmon frequency is 5.1 eV, which lies outside the spectral range of the HREELS experiment. Therefore, the decrease in the FWHM of the elastic peak for Pt layers thicker than 2 ML is attributed to the emergence of a discrete plasmon loss at high energy and the disappearance of the low energy plasmonlike loss continuum.

B. Growth of Pt overlayers on ZnO(0001)

The growth of Pt films on the ZnO(0001) surface was also examined in this investigation. The HREEL spectrum of the clean (0001) surface is shown in the lower portion of Fig. 5. As was the case for ZnO(000 $\bar{1}$), there is an intense loss at 67.0 meV, corresponding to the surface optical phonon and a phonon-phonon combination structure extending to higher

loss energies with maxima at integral multiples of the phonon fundamental. Comparison of the HREEL spectra of the clean (000 $\bar{1}$) and (0001) surfaces shows that the intensity of the phonon fundamental relative to that of the elastic peak is much less for the (0001) surface than for the (000 $\bar{1}$) surface [0.35 for the ZnO(0001) vs 0.68 for the ZnO(000 $\bar{1}$)]. Apparently, the conduction electrons provide a higher degree of screening of the oscillating dipole of the phonon vibration for ZnO(0001) compared to ZnO(000 $\bar{1}$). This result indicates that there is an electron accumulation layer on the ZnO(0001) surface. Clearly the electronic properties of the two surfaces, as evidenced by the HREEL spectra, are different. As will be shown below, these differences may be responsible for variations in the interaction of Pt films with the two surfaces.

In contrast to ZnO(000 $\bar{1}$), the deposition of submonolayer amounts of Pt on ZnO(0001) resulted in dramatic changes in the electronic properties of the surface. For Pt coverages in the range of 0.1–0.5 ML the surface region of the sample became insulating, thereby disrupting the HREELS analysis. HREEL spectra collected in this coverage regime were found to be highly irreproducible and characterized by an intense, narrow elastic peak due to reflection of electrons off the electrostatic field of the charged sample. This rather dramatic change in the conductivity of the ZnO sample upon Pt deposition is consistent with the formation of a surface depletion region in the oxide and implies that charge has been transferred from the ZnO substrate to the deposited Pt atoms. As will be discussed below, this charge transfer can be described in terms of the formation of a Schottky barrier at the interface.

It was found that electrostatic charging of Pt-covered ZnO(0001) could be alleviated by illuminating the sample with visible light. This procedure allowed HREEL spectra of the (0001) surface covered with 0.1–0.5 ML of Pt to be obtained. Although more detailed studies are required in order to determine the exact effect of visible light on the electronic properties of the Pt-covered surface, it is likely that the incident photons provided sufficient energy to excite electrons from the metal conduction band into the conduction band of the ZnO substrate or across the band gap of the oxide itself.

As noted above, the charging phenomenon persisted for Pt coverages up to 0.5 ML. For higher coverages, sample charging did not occur during the collection of HREEL spectra. A coverage of approximately 0.5 ML corresponds to the percolation limit of a two-dimensional overlayer, assuming random deposition of particles on a close-packed, hexagonal array or coalescence of Pt islands with a fixed number of nucleation sites.¹⁷ Thus, at this coverage there is a conduction path to the edge of the sample (which is in contact with the grounded sample holder) via the deposited Pt layer. This prevents the build-up of charge in the surface layer.

HREEL spectra of ZnO(0001) recorded following deposition of 0.5, 1.0, 2.0, and 3.0 monolayers of Pt are shown in the upper portion of Fig. 5. As was the case for ZnO(000 $\bar{1}$), there are changes in the intensity of the phonon peak relative to that of the elastic peak, and the FWHM of the elastic peak as the Pt coverage was increased. These quantities are plotted

vs Pt coverage for all experimentally measured overlayer thicknesses in Figs. 3(b) and 4(b), respectively.

The ratio of the intensity of the phonon peak to that of the elastic peak vs Pt coverage for deposition on ZnO(0001) is displayed in Fig. 3(b). Comparison of these data to the analogous data obtained from ZnO(000 $\bar{1}$) [Fig. 3(a)] reveals some significant differences. The most noticeable variation is that the ratio of the intensity of the phonon to elastic peak initially increased with Pt coverage for ZnO(0001), while it decreased monotonically for ZnO(000 $\bar{1}$). The ratio for the clean (0001) surface was 0.35; it increased to 0.58 for a Pt coverage of 0.1 ML and then rapidly fell to nearly zero as the coverage was increased to 3 ML. Since the Pt layer should shield the phonon mode from the scattered electrons for all Pt coverages, as was the case for ZnO(000 $\bar{1}$), this result was somewhat unanticipated. It is consistent, however, with transfer of charge from the oxide to the metal. This charge transfer reduces the number of free carriers in the surface region of the oxide giving rise to the charging phenomena described above. Since the free charge carriers in the oxide also shield the oscillating dipole of the phonon vibration, a reduction in their number increases the cross section for excitation of the phonon mode. For Pt coverages greater than 0.5 ML the reduction in the excitation cross section of the phonon mode due to the decrease in the number of free carriers in the oxide is offset by the shielding effect of the Pt layer and the phonon intensity begins to decrease.

Figure 4(b) shows that when Pt was deposited on ZnO(0001), the FWHM of the elastic peak remained unchanged from the clean surface value for Pt coverages up to approximately 0.6 ML. At this point the FWHM rapidly increased and reached a maximum of 23.8 meV at an overlayer thickness of 1.0 ML. The resolution then improved and nearly recovered to the clean surface value for a 2 ML film. Recall that for ZnO(000 $\bar{1}$), the FWHM increased rather slowly and nearly linearly for coverages up to 2.0 ML, where it achieved its maximum value. These differences further suggest that the nature of Pt-ZnO interaction varies between the two surfaces. It is interesting that on ZnO(0001) the Pt coverage where the rapid increase in the FWHM began is close to the percolation threshold for the metal layer.

C. Thermal stability of Pt overlayers

The thermal stability of Pt films on the polar surfaces of ZnO was also studied using HREELS. In these experiments samples covered with a 3 ML Pt film were heated to a series of progressively higher temperatures, at which point they were quenched to 100 K and HREEL spectra were collected. Figure 6 shows a representative sample of the data collected following annealing of a 3 ML Pt film on ZnO(0001). All of the data which were obtained from the annealing studies of Pt films on both surfaces are summarized in Fig. 7, which displays the ratio of the phonon intensity to that of the elastic peak following annealing of a 3 ML Pt film on both ZnO(000 $\bar{1}$) and ZnO(0001).

The data for ZnO(000 $\bar{1}$) in Fig. 7 shows that for temperatures less than 600 K, the phonon-elastic peak intensity ratio remained constant at 0.02. However, for annealing temperatures greater than 600 K, the ratio rapidly increased. Af-

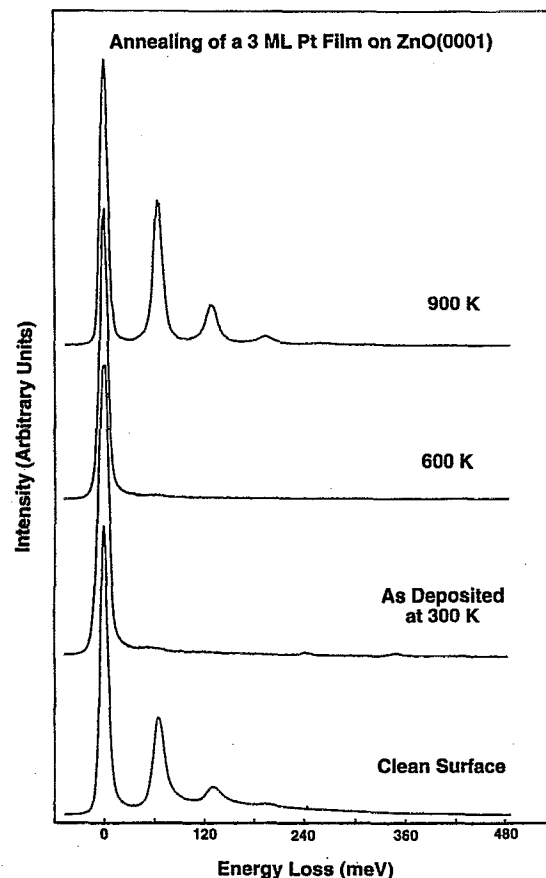


FIG. 6. HREEL spectra of a 3 ML Pt film on ZnO(0001) as a function of annealing temperature.

ter annealing the sample at 1000 K, the ratio was 0.54, a value slightly lower than that obtained from the clean surface. This increase in the relative phonon intensity for temperatures above 600 K is consistent with the coalescence of the two-dimensional Pt layer into three-dimensional particles, resulting in the exposure of portions of the ZnO(000 $\bar{1}$) surface. This result is consistent with the AES studies of Roberts and Gorte.⁷ The recovery of the normalized phonon intensity to nearly that of the clean surface suggests that a significant fraction of the ZnO surface is exposed, which in turn implies that the size of the Pt particles following agglomeration is relatively large. By comparison with the results of Roberts and Gorte, the particles formed by annealing the 3 ML film were estimated to be ~ 18 nm in diameter with a number density of $\sim 4 \times 10^{10}/\text{cm}^2$ (Ref. 7).

As is also shown in Fig. 7, the trend in the phonon intensity in the HREELS spectra upon annealing Pt-covered ZnO(0001) was qualitatively similar to that obtained from the ZnO(000 $\bar{1}$). This indicates that the Pt layers on ZnO(0001) also coalesce into particles upon heating. The onset of particle formation on the (0001) surface appeared to occur at approximately the same temperature as on the (000 $\bar{1}$) surface, but agglomeration of the Pt occurred more readily on this surface as evidenced by the more rapid reappearance of the ZnO phonon. It is also important to note that following annealing of Pt-covered ZnO(0001) to 1000 K, the

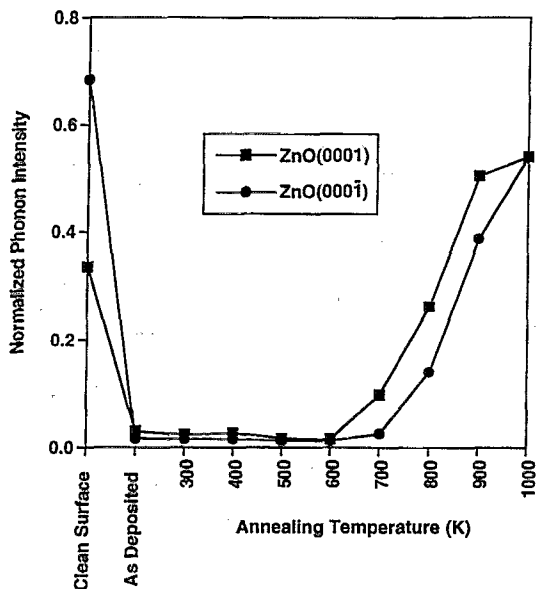
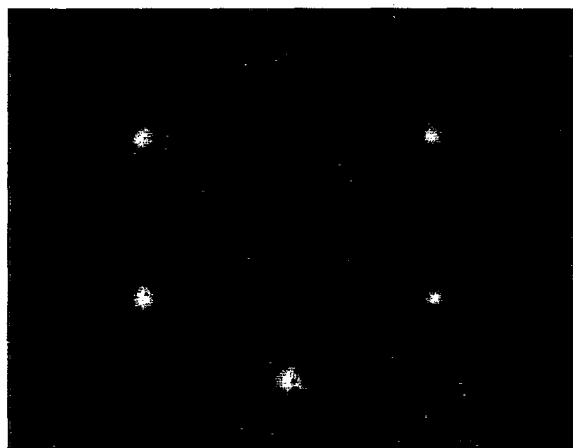


FIG. 7. Ratio of the intensity of the phonon peak in the HREEL spectrum to that of the elastic peak as a function of annealing temperature for ZnO(0001) and ZnO(0001̄) covered with 3 ML Pt films. Squares represent data from the Pt/ZnO(0001) system, whereas the circles correspond to data for Pt/ZnO(0001̄).

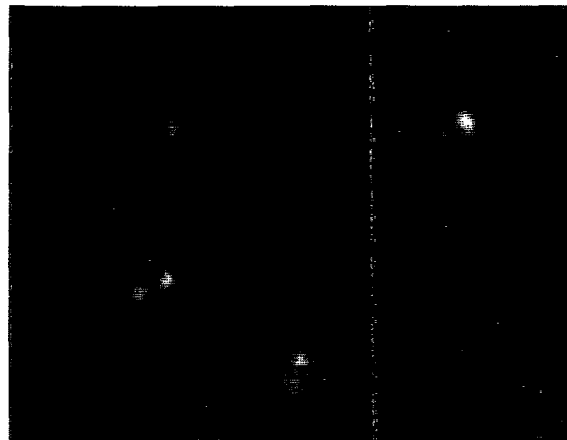
phonon-elastic peak intensity ratio was 0.54, a value significantly greater than that obtained from the clean surface (0.35). This result indicates that the Pt particles interact strongly with ZnO(0001) and that this interaction is similar to that of the two-dimensional films, i.e., there is charge transfer from the oxide to the metal which reduces shielding of the phonon.

D. LEED analysis

LEED was used to further characterize the structure of the Pt layers on ZnO(0001) and ZnO(0001̄). The LEED results from the two surfaces were nearly identical, so only those from the (0001) surface are presented here. Figure 8(a) shows the LEED pattern of clean ZnO(0001) acquired using an incident electron beam energy of 120 eV. The LEED pattern displays hexagonal symmetry as is expected for this surface, which consists of a hexagonal array of Zn²⁺ cations with a nearest-neighbor spacing of 3.25 Å. This pattern is in excellent agreement with those that have been reported previously for this surface.^{18,19} A slight amount of background intensity was also present, which may have been caused by diffuse scattering from steps and other defects on the surface.¹⁹



(a)



(c)



(b)

FIG. 8. LEED patterns of (a) clean ZnO(0001), (b) 5 ML of Pt film on ZnO(0001) at 300 K, and (c) following annealing of the film in (b) at 900 K. All patterns were collected using a primary beam energy of 120 eV.

LEED patterns of the ZnO(0001) surface as a function of Pt coverage were measured. The hexagonal pattern due to the ZnO(0001) substrate was observed for Pt coverages up to 1.0 ML, although it became less intense as the overlayer thickness was increased. Increasing the Pt layer thickness to 2 ML resulted in the emergence of a new hexagonal diffraction pattern which can be attributed to the Pt layer. The fact that this pattern was not completely developed until a coverage of 2 ML suggests that the first monolayer may be somewhat disordered.

The LEED pattern obtained at a beam energy of 120 eV for a 5.0 ML Pt overlayer is shown in Fig. 8(b). This pattern is similar to that obtained for a 2 ML film, but the spots are slightly sharper. Comparison of the hexagonal LEED patterns of the clean and metal-covered surfaces reveals that the spacing of the spots is larger in the pattern obtained from the Pt-covered surface. This result demonstrates that although the Pt layer is well ordered, it is not pseudomorphic with the ZnO(0001) substrate. Analysis of the LEED pattern to determine the real-space nearest-neighbor distance in the Pt layer yields a value of 2.71 Å. This is close to the nearest-neighbor spacing for a Pt(111) surface of 2.77 Å, indicating that the overlayer is relatively unstrained despite the lattice mismatch between ZnO and Pt. Previous TEM results of Roberts and Gorte for Pt films on ZnO(0001) indicated that the hexagonal array of the deposited Pt atoms was rotated 30° relative to that of the substrate.⁷ The LEED results in Figs. 8(a) and 8(b) clearly show that for the Pt films produced in this study, this rotation was not present. It is difficult to determine what caused this difference between the two studies. One possibility is that the films produced by Roberts and Gorte were exposed to air before being characterized. The LEED results of this study are consistent, however, with those obtained previously for the interaction of Pd and Cu with ZnO.^{20,21}

In the previous section, it was demonstrated that the Pt films agglomerate to form particles upon annealing at temperatures above 600 K. The LEED pattern obtained after annealing the sample covered with 5 ML of Pt to 900 K is displayed in Fig. 8(c). This pattern contains two concentric hexagonal arrangements of spots. The inner hexagonal pattern is similar to that in Fig. 8(a) and is due to the ZnO substrate, while the outer pattern has the same spacing as that in Fig. 8(b) and can be assigned to the Pt. This result demonstrates that the Pt particles formed upon high-temperature annealing remain oriented with respect to the substrate. The observation of a hexagonal pattern for the particles also indicates they are relatively flat and have exposed Pt(111) surfaces which are parallel to the ZnO substrate. This pattern is similar to those obtained previously in LEED studies of Pd and Cu-covered ZnO surfaces.^{20,21}

IV. DISCUSSION

The HREELS results demonstrate that there are significant differences in the interaction of Pt overlayers with ZnO(0001) and ZnO(0001). In order to explain the experimental results and determine the extent to which electronic interactions at the interface influence the structure and electronic properties of the deposited films, it is useful to start by considering a model of the system consisting of two uniform,

noninteracting layers, one representing the ZnO substrate and the other the deposited Pt film. As previously described in detail by others,²²⁻³⁰ the HREEL spectrum of layered system such as this can be simulated using semiclassical dielectric theory. In this approach the electrons are considered to be classical particles, while the surface excitations are treated quantum mechanically. Within this framework, one can define a surface loss function, $P(\omega)$, which describes the probability that a scattered electron will lose energy $\hbar\omega$.²³ A HREEL spectrum can be calculated by integrating the surface loss function over all excitation wave vectors which scatter the electron into the acceptance angle of the spectrometer. This classical loss function is then temperature corrected using a Bose-Einstein distribution, self-convoluted to reproduce the multiple loss structure, and convoluted with an instrumental response function to take into account the finite energy resolution of the spectrometer. The details of this type of calculation can be found in a paper by Lambin *et al.*²³

For a layered system, the surface loss function depends on the frequency of the excitation, ω , the scattered wave vector, \mathbf{k} , and the overlayer thickness, d , and is related to the dielectric response of the target as follows:²⁶

$$P(\omega, \mathbf{k}, d) = \text{Im} \left[\frac{-1}{\epsilon_{\text{eff}}(\omega, \mathbf{k}, d) + 1} \right],$$

where $\epsilon_{\text{eff}}(\omega, \mathbf{k}, d)$ is the effective dielectric constant of the layered system. For a single Pt layer on a semi-infinite ZnO substrate, the effective dielectric function is given by²³

$$\epsilon_{\text{eff}}(\omega, \mathbf{k}, d) = \epsilon_{\text{Pt}}(\omega) \frac{\epsilon_{\text{Pt}}(\omega) \tanh(kd) + \epsilon_{\text{ZnO}}(\omega)}{\epsilon_{\text{ZnO}}(\omega) \tanh(kd) + \epsilon_{\text{Pt}}(\omega)},$$

where ϵ_{ZnO} and ϵ_{Pt} are the dielectric constants of ZnO and Pt, respectively. The ZnO substrate can be treated as an isotropic dielectric medium with a single classical oscillator. Hence, its dielectric function is²⁶

$$\epsilon_{\text{ZnO}}(\omega) = \epsilon_{\infty} + \frac{(\Delta\epsilon)(\omega_{\text{TO}}^2)}{\omega_{\text{TO}}^2 - \omega^2 - i\omega\gamma},$$

where ϵ_{∞} is the high-frequency dielectric constant, $\Delta\epsilon$ is the oscillator strength, ω_{TO} is the transverse optical phonon frequency, and γ is the damping constant of the oscillator. It was found that literature values of $\epsilon_{\infty}=3.75$, $\Delta\epsilon=5.0$, $\omega_{\text{TO}}=46.7$ meV, and $\gamma=1.49$ meV (Refs. 31,32) yielded a simulated HREEL spectrum in qualitative agreement with that obtained experimentally from the clean ZnO(0001) surface. A Gaussian peak with a FWHM of 9.9 meV was used as the instrumental response function in these simulations. The dielectric response of the Pt overlayer was calculated using a Drude model,³³

$$\epsilon_{\text{Pt}}(\omega) = 1 - \frac{\omega_p^2}{\omega \left(\omega - \frac{i}{\tau} \right)},$$

where ω_p is the plasmon frequency and τ is the relaxation time. Values of $\omega_p=5.1$ eV and $\tau=7.83 \times 10^{-15}$ were obtained from the literature.^{34,35}

Before presenting the results of the HREEL simulations, some limitations of the dielectric model should be addressed.

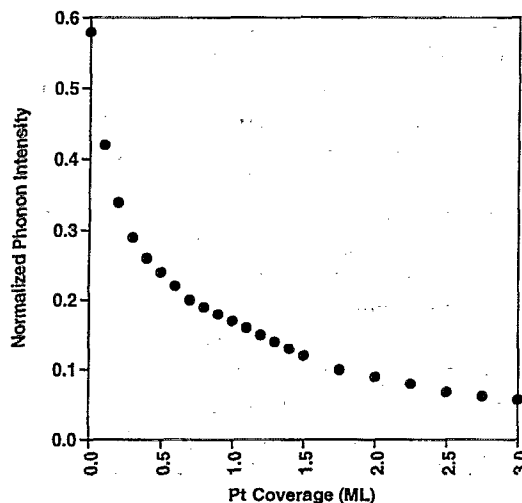


FIG. 9. Calculated ratios of the intensity of the phonon peak relative to that of the elastic peak as a function of Pt coverage. The ratios were calculated using the dielectric model described in the text.

The most important being that this model does not account for any direct interaction between the Pt and the ZnO such as coupling between the vibrational modes of the overlayer and the substrate or charge transfer between the layers. Also, the Pt overlayer was simulated as a continuous film with a uniform distribution of metal at all coverages. Obviously, this assumption is not valid for submonolayer coverages, since the Pt must be deposited as isolated Pt atoms or as islands. Despite these shortcomings, the calculation of HREEL spectra using dielectric theory is a valuable tool for predicting qualitative trends. Since the calculations are for noninteracting layers, any deviations from the simulated spectra observed in the experimental data may provide some insight into the nature of the Pt-ZnO interactions.

The results of the HREEL simulations for Pt overlayer thicknesses up to 3 ML are presented in Figs. 9 and 10, where the phonon intensity normalized to that of the elastic peak and FWHM of the elastic peak are plotted vs Pt coverage, respectively. The calculated value of the normalized phonon intensity for the clean ZnO surface was 0.58. This is somewhat less than the experimentally determined value for ZnO(000 $\bar{1}$) of 0.68. This discrepancy may be due to uncertainties in the values of the parameters used in calculating the effective dielectric constant.^{32,33} It might also indicate the presence of a small depletion layer on the (000 $\bar{1}$) surface. A reduction in the charge carrier concentration due to a surface depletion layer would result in less shielding of the phonon vibration and lead to an increase in the observed phonon intensity.

In contrast to the result obtained for ZnO(000 $\bar{1}$), the normalized phonon intensity obtained from the simulation deviates significantly from that obtained experimentally for ZnO(0001). The normalized phonon intensity of clean ZnO(0001) was 0.35 while the simulation predicts a value of 0.58. The decreased intensity of the phonon mode for ZnO(0001) relative to the simulation and ZnO(000 $\bar{1}$) can be attributed to shielding of the dipole of the phonon vibration by an accumulation layer of electrons near the (0001) sur-

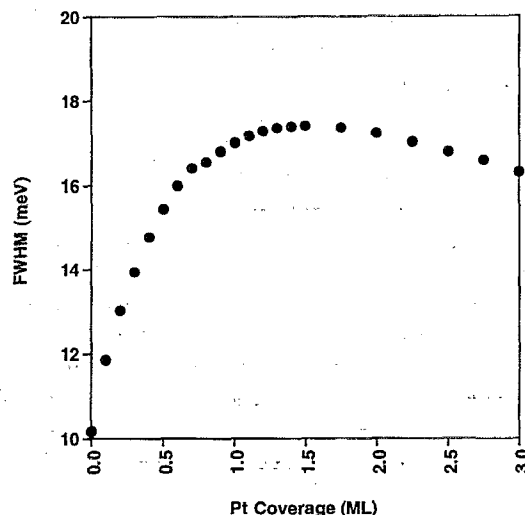


FIG. 10. Full-width at half-maximum of the elastic peak as a function of Pt coverage for the simulated HREEL spectra. The spectra were calculated using the dielectric model described in the text. A Gaussian peak with a FWHM of 9.9 meV was used as the instrumental response function in the simulation.

face. The large discrepancy between the measured and calculated phonon intensities indicates that the accumulation layer on the (0001) surface is quite large.

Upon "deposition" of Pt, the phonon intensity in the calculated spectra continually decreased as the Pt coverage was increased, as is shown in Fig. 9. In the simulation, shielding of the ZnO phonon mode by the conduction electrons in the Pt overlayer was nearly complete for a 3 ML Pt film. These results are in good agreement with those obtained experimentally from ZnO(000 $\bar{1}$), as shown in Fig. 3(a). This result supports the conclusion that the Pt grows in a nearly layer-by-layer fashion on this surface. The similarity between the spectra simulated using a noninteracting layer model and experiment also suggests that there is not a considerable amount of charge transfer at the Pt/ZnO(000 $\bar{1}$) interface. In contrast, the results obtained from the (0001) surface, presented in Fig. 3(b), deviate appreciably from the simulated spectra in the low coverage regime, indicating significant electronic interactions between the Pt film and this surface.

The FWHM of the elastic peak measured as a function of Pt coverage for the simulated data (see Fig. 10) also exhibits behavior which is qualitatively similar to that observed for ZnO(000 $\bar{1}$). The FWHM increased with increasing Pt overlayer thickness to a maximum value of 19.8 meV, then gradually returned to a value close to that of the clean ZnO surface. This result indicates that surface roughness is not the major cause of the decreased spectral resolution, since this factor was not included in the simulation. The increase in FWHM can be accounted for by convolution of the intense, plasmonlike loss continuum of the thin Pt film with the elastic peak. As is evident upon comparison of Fig. 4(b) with Figs. 4(a) and 10, the FWHM vs coverage results for Pt deposition on ZnO(0001) were very different from both the simulation and the experimental data for Pt/ZnO(000 $\bar{1}$). In

this case, no significant change in the FWHM of the elastic peak was observed below a Pt coverage of 0.6 ML. Beyond this point, rapid broadening was observed until the FWHM reached a maximum value of 23.8 meV for a Pt thickness of 1.0 ML. Further Pt deposition resulted in a decrease in the FWHM. This cusp-shaped curve which is sharply peaked at 1.0 ML provides further evidence that there is a strong electronic interaction between Pt and ZnO(0001). The constant value of the FWHM for coverages less than 0.6 ML can be attributed to the balancing of two effects, plasmonlike losses in the thin Pt film which tend to increase the FWHM and a reduction in the number of free carriers in the surface region of the oxide substrate which tends to decrease the FWHM. As the coverage of the Pt layer increases, the plasmon losses in the metal film begin to dominate and there is a sharp increase in the spectral FWHM.

The HREELS results obtained in this study, in conjunction with the simulated spectra, indicate that the vapor-deposited Pt films grow in a nearly layer-by-layer fashion. This is consistent with the AES and TEM studies of Roberts and Gorte.⁷ It is interesting that, in light of the fact that thermodynamics appears to favor the formation of Pt particles, the metal film grows layer-by-layer. The thermodynamic limit is demonstrated in the annealing studies which showed that, upon heating above 600 K, Pt films on both of the ZnO surfaces coalesced into particles. This suggests that Pt-Pt interactions are stronger than Pt-ZnO interactions. A similar effect has recently been reported by Ernst *et al.* for the interaction of Cu with ZnO(0001).³⁶ In that study it was found that vapor-deposited Cu formed two-dimensional islands on ZnO(0001) for coverages less than 0.5 ML. Annealing of these Cu films to temperatures in excess of 300 K resulted in agglomeration into large Cu particles. Coalescence occurred over a wide temperature range, but was complete by 800 K.

Ernst *et al.* proposed a simple kinetic model which is capable of explaining this result.³⁶ The basic premise of this model is that as long as no islands have nucleated in the second layer of the metal film, adsorbed atoms on the surface of a one atom thick metal island would migrate to the edge of the island and then down onto the substrate. This would maximize their nearest-neighbor interactions. Once islands have nucleated on the second layer, it would be more energetically favorable for isolated metal adatoms to migrate to the edge of the second layer metal islands, provided that the strength of the metal-metal interactions is greater than that of the metal-metal oxide interactions. The authors proposed that the onset of two-dimensional growth would occur above some critical coverage, θ_c , of monolayer thick metal islands. Presumably, the value of θ_c is determined by the rate at which adatoms migrate to island edges and down into the first layer and therefore depends on the energy barriers for diffusion on the metal surface and for migration from the second layer to the first layer.

There are many similarities between the results obtained for Pt and Cu and it appears that the model proposed by Ernst *et al.* for the Cu/ZnO(0001) system is applicable to the Pt/ZnO(0001) and Pt/ZnO(0001) systems as well. In particular, it provides a mechanism for the growth of two-

dimensional films, even though the thermodynamic limit is particle formation. There are some subtle differences, however, between the results obtained for Cu and those for Pt. Most important of these is the critical coverage of monolayer islands at which nucleation of metal islands in the second layer occurs (ie., the onset of three-dimensional growth). This critical coverage was found to be 0.5 ML for Cu on ZnO(0001),³⁶ while the results of this study indicate that for Pt on ZnO(0001) and ZnO(0001) θ_c is closer to 1 ML. Examination of the model reveals that this difference is consistent with the energy barrier for migration of metal atoms from the second layer of a metal island down into the first layer being smaller for Pt than for Cu. This is likely to be the case if Pt-ZnO interactions are stronger than Cu-ZnO interactions. The annealing behavior of the Cu and Pt films provides some evidence to support this conclusion. In particular the onset of agglomeration of Cu layers into large particles occurs near 300 K,³⁶ while for Pt layers the onset of agglomeration occurs at a much higher temperature, 600 K.

The observed transition of the ZnO(0001) from a semiconductor to an insulator upon deposition of very small quantities of Pt(0.1–0.5 ML) was somewhat surprising when first encountered. However, this result can be easily reconciled by considering the formation of a Schottky barrier. If a metal and an *n*-type semiconductor are brought into contact with one another, charge carriers are transferred from the valence band of the semiconductor to the metal in order to equalize their respective Fermi levels.³⁷ When this occurs, the bands of the semiconductor are bent upward and a region where the charge carrier concentration is severely depleted is formed in the surface region. Apparently, even for Pt coverages of less than 0.1 ML on ZnO(0001), the upward band-bending of the ZnO valence band is sufficient to cause a semiconductor-to-insulator transition in the surface region of the oxide. Upward band-bending accompanied by charge transfer from the oxide to the metal overlayer has also been observed in the case of Cu deposition on ZnO(0001).³⁸

The formation of a Schottky barrier is also consistent with the observed increase in the normalized phonon intensity upon deposition of 0.1 ML of Pt on ZnO(0001). As was shown in the results section, the (0001) surface contains an accumulation layer of charge carriers. This layer of charge carriers screens the surface phonon mode, causing a reduction in its intensity in the clean surface HREEL spectrum. Upon deposition of a small amount of Pt, localized Schottky barriers are formed. This reduces the amount of screening of the phonon oscillation by conduction electrons in the oxide and produces an increase in the normalized phonon intensity in the HREEL spectrum.

Perhaps the most significant result in this study is the demonstration of how interfacial structure can influence electronic interactions at metal/metal oxide interfaces. The experimental results did not provide any evidence for a significant amount of charge transfer at the Pt/ZnO(0001) interface. The trends in the HREEL spectra of Pt films deposited on ZnO(0001) were qualitatively similar to those predicted by a model consisting of two uniform, noninteracting dielectric layers. In contrast, Schottky barrier formation was observed upon deposition of Pt on ZnO(0001). Transfer of charge from

the oxide to the metal layer on this surface is sufficient to cause the surface region of the oxide to undergo a semiconductor-to-insulator transition. These differences are clearly related to the structure and electronic properties of the two ZnO surfaces. The (0001) surface contains equal numbers of cations and anions and has an electron accumulation layer, while the (000 $\bar{1}$) surface is primarily composed of anions and has a much lower concentration of charge carriers. The differences in the electronic interactions at the Pt/ZnO(000 $\bar{1}$) and Pt/ZnO(0001) interfaces may be responsible for the chemical reactivity variations observed by Roberts and Gorte.⁷ As noted earlier, these authors observed a 50 K downward shift in the CO desorption temperature for CO adsorbed on Pt film supported on ZnO(0001) compared to CO adsorbed on a Pt film supported on ZnO(000 $\bar{1}$).

V. CONCLUSIONS

HREELS and LEED were used to study the growth, structure, and electronic properties of thin Pt films on ZnO(000 $\bar{1}$) and ZnO(0001). It was found that vapor-deposited Pt grew epitaxially in nearly a layer-by-layer fashion on both surfaces. After deposition of approximately 2 ML of Pt, the layers exhibited hexagonal symmetry and had a lattice constant close to that of a Pt(111) surface. Despite the similarity in the growth mechanisms on the two surfaces, the HREELS results indicated that the interaction of Pt with ZnO(0001) is dramatically different than that with ZnO(000 $\bar{1}$). There was no evidence for significant electronic interactions between Pt and ZnO(000 $\bar{1}$). This was confirmed by a correspondence of the Pt/ZnO(000 $\bar{1}$) results with simulated HREEL spectra calculated using a noninteracting dielectric layer model. In contrast, HREEL spectra collected from the Pt/ZnO(0001) system deviated significantly from the model. The data in this case are consistent with transfer of electrons from the oxide to the deposited metal, resulting in the formation of a Schottky barrier at the interface. These results demonstrate the importance of local structure in determining electronic interactions at metal/metal oxide interfaces.

The two-dimensional Pt films formed by vapor deposition at low temperature were stable for annealing temperatures below approximately 600 K. Beyond this point, the Pt agglomerated to form relatively large particles. LEED demonstrated that the particles were oriented with respect to the ZnO substrate and had exposed Pt(111) surfaces.

ACKNOWLEDGMENTS

We gratefully acknowledge the financial support of the National Science Foundation (Grant No. CT S89-57056) and the Laboratory for Research on the Structure of Matter at the

University of Pennsylvania (National Science Foundation MRL Program, Grant No. DMR91-20668) for the use of its facilities. We would also like to thank Dr. N. J. DiNardo for many useful discussions and critical reading of this manuscript prior to its submission.

- ¹J. M. Vohs and M. A. Barteau, *Surf. Sci.* **176**, 91 (1986).
- ²J. M. Vohs and M. A. Barteau, *Surf. Sci.* **201**, 481 (1988).
- ³J. M. Vohs and M. A. Barteau, *J. Phys. Chem.* **91**, 4766 (1987).
- ⁴J. M. Vohs and M. A. Barteau, *J. Phys. Chem.* **93**, 8343 (1989).
- ⁵G. Zwicker, K. Jacobi, and J. Cunningham, *Int. J. Mass Spectrosc. Ion Processes* **60**, 213 (1984).
- ⁶S. Akhter, K. Lui, and H. H. Kung, *J. Phys. Chem.* **89**, 1958 (1985).
- ⁷S. Roberts and R. J. Gorte, *J. Phys. Chem.* **93**, 5337 (1990).
- ⁸A. N. Mariano and R. E. Hanneman, *J. Appl. Phys.* **34**, 384 (1963).
- ⁹J. I. Gersten, *Surf. Sci.* **92**, 579 (1980).
- ¹⁰J. I. Gersten, *Surf. Sci.* **97**, 206 (1980).
- ¹¹Y. Goldstein, A. Many, I. Wagner, and J. Gersten, *Surf. Sci.* **98**, 599 (1980).
- ¹²A. Many, I. Wagner, A. Rosenthal, J. I. Gersten, and Y. Goldstein, *Phys. Rev. Lett.* **46**, 1648 (1981).
- ¹³H. Ibach, *Phys. Rev. Lett.* **24**, 1416 (1970).
- ¹⁴W. T. Petrie and J. M. Vohs, *Surf. Sci.* **245**, 315 (1991).
- ¹⁵W. T. Petrie and J. M. Vohs, *J. Vac. Sci. Technol. A* **11**, 2169 (1993).
- ¹⁶L. H. Dubois, G. P. Schwartz, R. E. Camley, and D. L. Mills, *Phys. Rev. B* **29**, 3208 (1984).
- ¹⁷D. Stauffer, *Introduction to Percolation Theory* (Taylor and Francis, Philadelphia, 1985), p. 15.
- ¹⁸H. van Hove and R. Leysen, *Phys. Status Solidi A* **9**, 361 (1972).
- ¹⁹M. Grunze, W. Hirschwald, and D. Hofmann, *J. Cryst. Growth* **52**, 241 (1981).
- ²⁰H. Jacobs, W. Mokwa, D. Kohl, and G. Heiland, *Surf. Sci.* **160**, 217 (1985).
- ²¹C. T. Campbell, K. A. Daube, and J. M. White, *Surf. Sci.* **182**, 158 (1987).
- ²²P. Lambin, J. P. Vigneron, and A. A. Lucas, *Solid State Commun.* **54**, 257 (1985).
- ²³P. Lambin, J. P. Vigneron, and A. A. Lucas, *Phys. Rev. B* **32**, 8203 (1985).
- ²⁴T. Conard, J. M. Vohs, P. A. Thiry, and R. Caudano, *Surf. Interface Anal.* **16**, 446 (1990).
- ²⁵P. A. Thiry, M. Liehr, J. J. Pireaux, and R. Caudano, *J. Electron Spectrosc. Relat. Phenom.* **39**, 69 (1986).
- ²⁶P. A. Thiry, M. Liehr, J. J. Pireaux, and R. Caudano, *Phys. Scr.* **35**, 368 (1987).
- ²⁷J. J. Pireaux, P. A. Thiry, R. Sporken, and R. Caudano, *Surf. Interface Anal.* **15**, 189 (1990).
- ²⁸B. G. Frederick, G. Apai, and T. N. Rhodin, *J. Electron Spectrosc. Relat. Phenom.* **54/55**, 415 (1990).
- ²⁹B. G. Frederick, G. Apai, and T. N. Rhodin, *Phys. Rev. B* **44**, 1880 (1991).
- ³⁰B. G. Frederick, G. Apai, and T. N. Rhodin, *Surf. Sci.* **277**, 337 (1992).
- ³¹R. J. Collins and D. A. Kleinmann, *J. Phys. Chem. Solids* **11**, 190 (1959).
- ³²E. C. Heltemes and H. L. Swinney, *J. Appl. Phys.* **38**, 2387 (1967).
- ³³H. Ibach and D. L. Mills, *Electron Energy Loss Spectroscopy and Surface Vibrations* (Academic, New York, 1982), p. 79.
- ³⁴*Handbook of Optical Constants of Solids II*, edited by E. D. Palik (Academic, San Diego, 1991), p. 318.
- ³⁵N. W. Ashcroft and N. D. Mermin, *Solid State Physics* (Saunders, Philadelphia, 1976), pp. 4–10.
- ³⁶K. H. Ernst, A. Ludviksson, R. Zhang, J. Yoshihara, and C. T. Campbell, *Phys. Rev. B* **47**, 13 782 (1993).
- ³⁷C. Kittel, *Introduction to Solid State Physics*, 6th Ed. (Wiley, New York, 1986), pp. 548–549.
- ³⁸S. V. Didziulis, K. D. Butcher, S. L. Cohen, and E. I. Solomon, *J. Am. Chem. Soc.* **111**, 7110 (1989).